

Magnetic and Dielectric Properties of Low Temperature co-fired Na-Ta co-doped M-type Barium Ferrites

Shuai Wang^{1,2}, Jie Li^{1*}, Yiheng Rao¹, Yan Yang^{1,3}, Gongwen Gan¹,
Dongbin Tian⁴, Sheng Li⁵, and Huaiwu Zhang¹

¹School of Electronic Science and Engineering, University of Electronic Science and Technology of China, Chengdu 610054, China

²National Engineering Research Center of Electromagnetic Radiation Control Materials, University of Electronic Science and Technology of China, Chengdu 611731, China

³The Collaborative Innovation Center of Integrated Computation and Chip Security, Chengdu University of Information Technology, Chengdu 610225, China

⁴Xinyun Electronic Company, China Zhenhua Electronics Group Company, Guiyang 551018, China

⁵YunKe Branch Company, China Zhenhua Electronics Group Company, Guiyang 551018, China

(Received 26 July 2018, Received in final form 30 September 2018, Accepted 3 December 2018)

Na-Ta ions co-doped M-type barium ferrites, $\text{BaFe}_{12-2x}(\text{NaTa})_x\text{O}_{19}$, were synthesized at low temperature by the solid-state method. Na-Ta ion could occupy crystalline sites but not change the phase formation of barium ferrite. SEM images showed that samples had the regular and hexangular shape with 1-2 μm size. With the increase of Na-Ta, saturation magnetization (M_s) obviously decreased from 57.5 emu/g to 37.6 emu/g, and the coercivity (H_c) decreased from 4156 Oe to 2069 Oe. For dielectric properties, the real part permittivity (ϵ') increased when x from 0.0 to 0.3, reaching the maximum value in a range frequency of 10 MHz-500 MHz, while decreasing when $x=0.4$. This material would be applied in electronic devices using LTCC technology.

Keywords : barium ferrite, Na-Ta co-doping, magnetic properties, dielectric properties

1. Introduction

As one of the important classes of permanent magnetic materials, M-type barium ferrite ($\text{BaFe}_{12}\text{O}_{19}$) have relatively large saturation magnetization (M_s) and high coercivity (H_c) as well as excellent chemical stability and corrosion resistivity [1]. It has frequently been used as hard magnetic magnets and magnetic recording media. And a wide span of other applications in electro-mechanical and electronic devices, such as circulator and isolator, it only need to adjust related properties to meet the requirements of devices [2]. Ions substitution has been carried out for moderate coercivity or magnetic permeability [3]. Meanwhile, multilayer devices are the most popular in electronic information field. To meet these needs, low temperature co-fired ceramics (LTCC) technology, which was used to fabricate multilayer devices in the past, has been investigated to reduce the size of electronic devices [4].

M-type barium ferrites have been applied in several ways. Now, to enlarge the wide range of applications, researchers have explored the substitutions for various trivalent cations for the Fe^{3+} ion in barium ferrites. The Fe^{3+} ions can be replaced by an assortment of trivalent cations such as Sc^{3+} , In^{3+} and Al^{3+} etc. [5, 6], or divalent-tetravalent cations pairs such as La-Co, Co-Ti, Ni-Ti and so on [7-9]. In our research, we chose Na^+ ion and Ta^{5+} ion to co-doped Fe^{3+} ion in M-type barium ferrites at low temperature, to study the structure and magnetic properties. Meanwhile, low melting point Bi_2O_3 additive was added to lower the sintering temperature, to apply the ferrite in LTCC technology.

2. Experiment

With analytical grade BaCO_3 , Fe_2O_3 , Na_2CO_3 and Ta_2O_5 as raw materials and by means of solid state reactions, Na^+ and Ta^{5+} ions co-doping M-type barium ferrites were synthesized, in the advantage of the chemical formula $\text{BaFe}_{12-2x}(\text{NaTa})_x\text{O}_{19}$, $x=0.0, 0.1, 0.2, 0.3, 0.4$ and 0.5 . Those raw materials were in powder form. They were

©The Korean Magnetism Society. All rights reserved.

*Corresponding author: Tel: +86-028-83203793

Fax: +86-028-83207063, e-mail: lijie@uestc.edu.cn

milled in a Teflon ball mill for 16 h with zirconia balls, and deionized water as the grinding media. The mixed material was dried and then pre-sintered at 1100 °C for 4 h in air. The pre-sintered one was further milled for 12 h in deionized water with 2.5 wt% Bi₂O₃ as sintering aid. After being dried, the powder was granulated by adding 8 wt% of polyvinyl alcohol (PVA) as a binder and pressed into some 2-3 mm thick-plate samples, which were then sintered at 900 °C for 6 h.

The phase compositions of the samples were pointed out by an X-ray diffractometer (XRD, DX-2700, Haoyuan Co.) with Cu K α radiation. The microstructures of the samples were characterized under a scanning electron microscope (SEM, JEOL, JSM-6490). Magnetization hysteresis loops were measured by a vibrating sample magnetometer (VSM, MODEL, BHL-525), from which the saturation magnetization and coercivity were calculated. The real part of dielectric permittivity was measured by Agilent 4991 impedance analyzer.

3. Results and Discussion

Figure 1 firstly presents the XRD patterns of 900 °C sintered samples with different levels of Na⁺ and Ta⁵⁺ ions substitutions from $x=0.0$ to 0.4. It was obviously found that the M-type hexagonal phase was formed in all the samples. Moreover, it was clearly found that only the single barium hexagonal phase in those samples with different substitution amount. This indicated that single phase M-type barium ferrite was successfully synthesized with Na-Ta co-doped at a low temperature 900 °C, while the doping did not affect the structure of the M-type barium ferrite.

Secondly, Fig. 1 showed that the diffraction peaks of

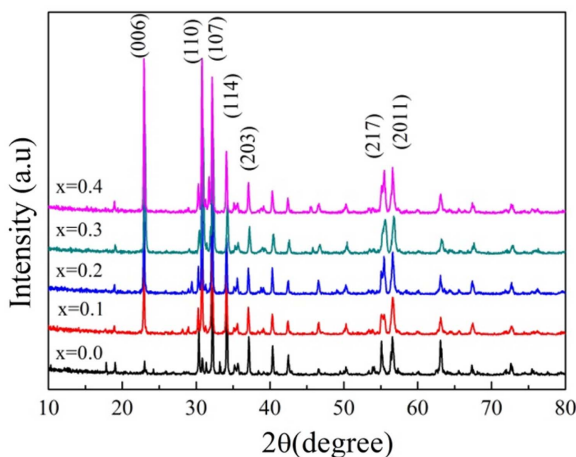


Fig. 1. (Color online) XRD patterns of samples with different Na-Ta contents.

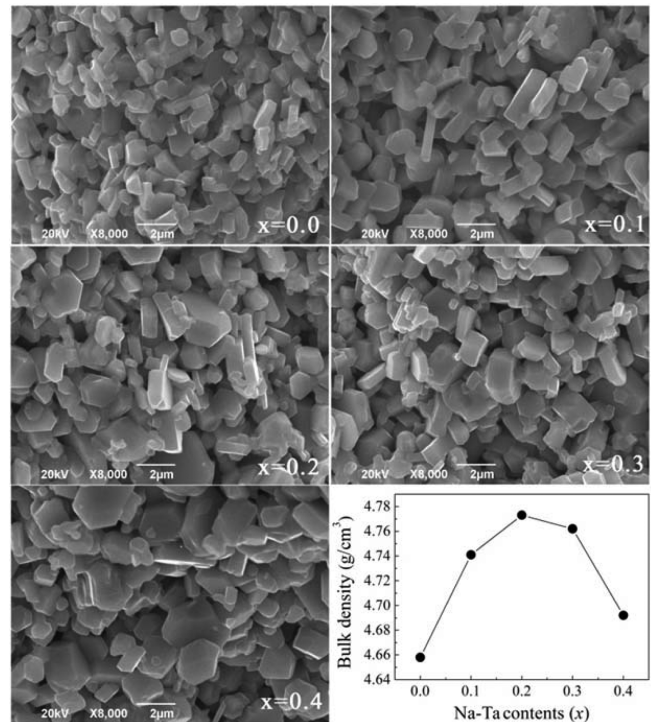


Fig. 2. SEM images and bulk density of samples with different Na-Ta contents.

$x=0.1$ sample were lower than other samples. This was because Na-Ta ions doped the different lattice sites. When Na-Ta doped contents were few, the lattice orientation (006) was weak. With the increasing of the doped contents, the orientation (006) became stronger. Hence, the diffraction peaks of $x=0.1$ sample were lower than other ones.

Figure 2 presented the SEM images of the samples sintered at 900 °C with different Na-Ta ion amounts. At first, It was shown that all the grain morphology of the samples exhibited a regular hexagonal structure. The grain sizes of samples were from 1 μm to 2 μm . Meanwhile, the grain sizes became bigger as the co-doping amounts of Na-Ta ions increased. The Na⁺ ion radius is 1.02 Å and Ta⁵⁺ ion radius is 0.64 Å [10]. Compared to Fe³⁺ ions with a radius of 0.645 Å, Ta⁵⁺ ions were similar, but Na⁺ ions were much larger. When Na-Ta ions doped M-type barium ferrite, it could cause lattice distortion, and then the lattice constant would raise with the increase of Na-Ta ions substitution. Correspondingly, this might also be the reason for the increase in grain size.

Secondly, as shown in Figure 2, the bulk density of the samples also increased when the amounts of Na-Ta ions substitutions raised. This was because that Na and Ta atoms have higher relative atomic mass than Fe atoms. The maximum reached when the doping amount is $x=0.2$,

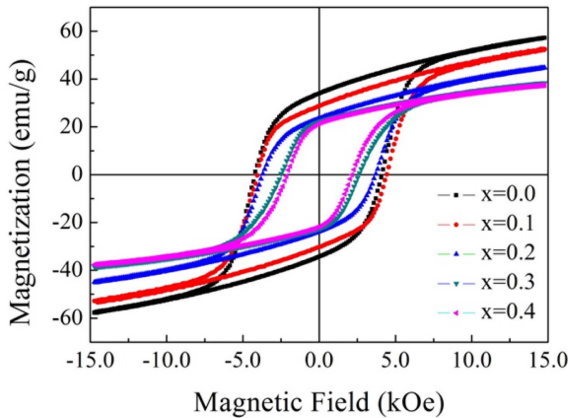


Fig. 3. (Color online) Room temperature hysteresis loops of samples.

and then decreased. Due to the excessive doping of Na and Ta ions, grain size started to increase. As a result, the pores enlarged to decrease the compactness, in turn, which reduced its bulk density. Once the magnetic properties and dielectric properties met the requirements, good compactness and fewer pores could be expected. Additionally, as shown in Fig. 2, with the increase of Na-Ta ions co-doping contents, the grain size increased, which brought saturation magnetization increase but coercivity decrease. Meanwhile, when the doping amount of Na-Ta ions is $x=0.2$, the density of these samples reached the maximum density, so $x=0.2$ is a more proper amount of addition.

Figure 3 showed the magnetic hysteresis loops of the samples, with saturation magnetization and coercivity as a function of Na-Ta doped. Hysteresis loops still indicated samples with hard magnetic properties. The changes of the saturation magnetization (M_s) and coercivity (H_c) with different doping amounts of Na-Ta ions were also presented in Fig. 4. It was shown that while Na-Ta ions

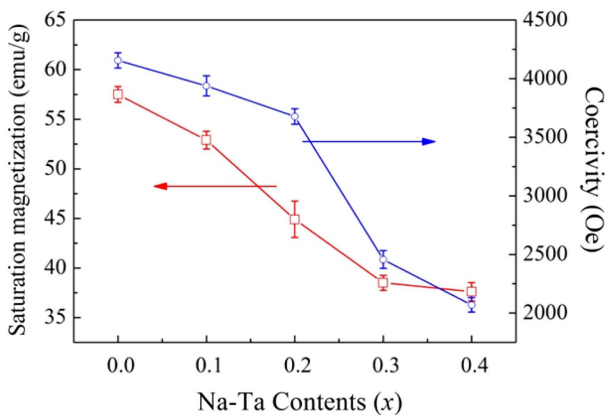


Fig. 4. (Color online) Saturation magnetization and coercivity as a function of Na-Ta doped.

contents increased from $x=0.0$ to 0.4, the saturation magnetization (M_s) decreased from 57.5 emu/g to 37.6 emu/g, and the coercivity (H_c) decreased from 4156 Oe to 2069 Oe. Meanwhile, although the Na-Ta doping did not achieve the transition of the M-type barium ferrite from hard to soft magnetic, it changed its magnetic properties yet. The saturation magnetization of ferrite was mainly determined by the chemical composition and the total magnetic moment of the materials, as well as their density and the grain size [11-13]. From the above three aspects, the changing reason in saturation magnetization of the samples could be strongly explained.

Firstly, In the M-type barium ferrite, Fe^{3+} ions occupied five different lattice positions: three octahedral sites $12k$, $2a$ and $4f_2$, one tetrahedral site $4f_1$, and one bipyramidal site $2b$ [14]. When Na-Ta ions were substituted for Fe ions, different lattice positions would be occupied depending on the doping amount and the characteristics of the ions themselves. The magnetic moment of Fe^{3+} ions was $5 \mu_B$, the magnetic moment of Na^+ ions and Ta^{5+} ions was $0 \mu_B$, which was smaller than the magnetic moment of Fe^{3+} ions. Therefore, Na-Ta ions doped would reduce the total magnetic moment of the materials. This was one of the main reasons why the saturation magnetization of the material decreased with the increase of Na-Ta ions doped.

Secondly, For the M-type barium ferrite, the magnetic source of the material was derived from the super-exchange effect between the metal ions in the material, as well as through the super-exchange effect of O^{2-} ions. The strength of super-exchange didn't only depend on the distance between metal ions, but also the number and state of 3d electrons in metal ions. The substitution of Fe ions by non-magnetic Na-Ta ions made the $Fe^{3+}-O^{2-}-Fe^{3+}$ exchange interactions effect weaker. In turn, this caused the saturation magnetization of the material to decrease.

At last, like mentioned above, the density and the grain size also affected the saturation magnetization of the material. As shown in Fig. 2, the grain size increased with the increase of the doping amounts of Na-Ta ions, the pores would increase as well. Hence, reduced compactness of the sample was the third reason to decrease saturation magnetization of the material.

The coercive force of the material was proportional to the constant of magneto-crystalline anisotropy of the material and inversely proportional to its saturation magnetization. For the M-type barium ferrite, the coercive force could be expressed as $H_c \approx (2 \cdot K) / (\mu_0 \cdot M_s)$, where K , μ_0 , M_s represented magneto-crystalline anisotropy constant, initial permeability and saturation magnetization. Magneto-crystalline anisotropy was mainly affected by electron spin and domain wall displacement [14]. Na-Ta ions

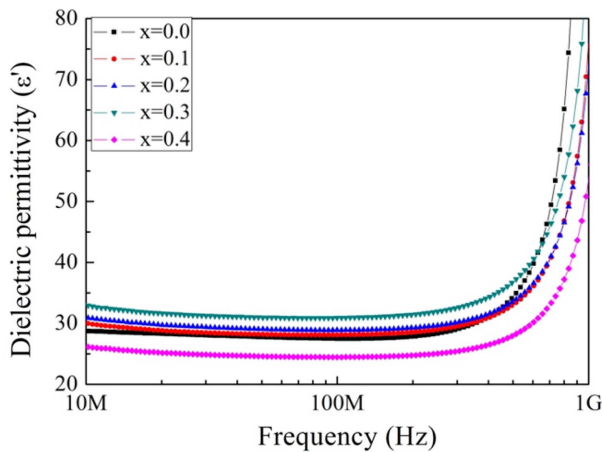


Fig. 5. (Color online) The real part of the dielectric permittivity (ϵ') of the samples with different doping amounts of Na-Ta ion.

doping made the grain size increase, and then the effect of grain boundary resistance to domain wall displacement would become weaker, which indicated magneto-crystalline anisotropy constant got lower. In addition, the effect of magneto-crystalline anisotropy on coercive force was much greater than the effect of saturation magnetization on coercive force. Therefore, the coercive force of the samples would decrease as the added amount of Na-Ta increased.

In summary, the magnetic properties of the material could be controlled by changing the doping amount of Na-Ta ions to meet the expectation. In this study, both the saturation magnetization and the coercive force of the samples decrease with the increase of the amount of Na-Ta ions.

The real part of the dielectric permittivity (ϵ') of the samples with different doping amounts of Na-Ta ion were measured in a range frequency of 10 MHz-500 MHz, as shown in Fig. 5. It could be found that the real part of the dielectric permittivity first increased when x from 0.0 to 0.3, reached the max value when $x=0.3$, but decreased when $x=0.4$. Considering the dielectric polarization problem from a microscopic point of view, the causes of polarization could be divided into the following four types: electronic displacement polarization, ionic polarization, polar orientational polarization and space charge polarization. According to the Clausius equation, the dielectric constant of the material can be expressed as $\epsilon=1+(N*\alpha/\epsilon_0) * (E_i/E)$, where N , α , ϵ_0 , E_i and E represent the number of molecules per unit volume of the material, polarizability, vacuum dielectric constant, effective electric field and the average of macro electric field. At the same time, α is the sum of polarizability produced by four

different polarization mechanisms. The dielectric constant of the material was related to the N value of the material which could be expressed by the sample density. This can be considered as a greater density meaning that there are more ferrite particles and fewer pores per unit volume, corresponding to a higher dielectric constant [15, 16]. According to Fig. 2, the change in dielectric constant of the sample had the same trend as the sample density that both of them increased first and then decreased. So the possible reason for the change in the dielectric constant of the sample might be the change in the density of the sample. Furthermore, in the high frequency field, the dielectric properties of ferrites were mainly attributed by the polarization of atomic and electronic in grain, and the content of Fe^{2+} ions plays an important role [17-19]. Since Fe^{2+} ions had one more electron than Fe^{3+} ions, Fe^{2+} ions were more likely to be polarized with respect to Fe^{3+} ions and thus had a greater polarizability. Although it was expected that only Fe^{3+} ions were present in all samples, due to various reasons, Fe^{2+} ions would still be produced. In particular, the increase in grain size and inhomogeneity would cause the content of Fe^{2+} ions rising, resulting in an increase in dielectric constant. Therefore, the increase of the dielectric constant at the beginning may be related to the increase of the grain size and the amount of Fe^{2+} ions in the samples.

4. Conclusion

In this study, Na-Ta ions co-doped M-type barium ferrite were successfully synthesized at low temperature by the solid-state method. While Na-Ta contents increased from $x=0.0$ to 0.4, the saturation magnetization (M_s) decreased from 57.5 emu/g to 37.6 emu/g, at the same time that the coercivity (H_c) reduced from 4156 Oe to 2069 Oe. For dielectric properties, the real part permittivity increased when x changed from 0.0 to 0.3, until reaching the max value in a range frequency of 10 MHz-500 MHz, and then decreased when $x=0.4$. By adjusting the doping amount, ferrite materials can be made out to meet a certain requirement. The result of our research can be used to prepare devices under LTCC technology.

References

- [1] Y. Y. Meng, M. H. He, Q. Zeng, D. L. Jiao, S. Shukla, R. V. Ramanujan, and Z. W. Liu, *J. Alloys Compd.* **220-225**, 583 (2014).
- [2] G. F. Liu, Z. D. Zhang, F. Dang, C. B. Cheng, C. X. Hou, and S. D. Liu, *J. Magn. Magn. Mater.* **55-62**, 412 (2016).
- [3] J. Li, H. W. Zhang, Y. N. Liu, Q. Li, T. C. Zhou, and H.

- Yang, *Appl. Phys. a-Mater.* **525-532**, 119 (2015).
- [4] M. A. Rafiq, M. Waqar, T. A. Mirza, A. Farooq, and A. Zulfiqar, *J. Electro. Mater.* **241-246**, 46 (2017).
- [5] D. Lisjak, M. Bukovec, and K. Zupan, *J. Nanopart. Res.* **18** (2016).
- [6] D. Chen, Y. Liu, Y. Li, K. Yang, and H. Zhang, *J. Magn. Magn. Mater.* **65-69**, 337 (2013).
- [7] Y. Wang, Y. L. Liu, J. Li, Q. Liu, H. W. Zhang, and V. G. Harris, *Aip. Adv.* **6** (2016).
- [8] J. Li, H. W. Zhang, Y. N. Liu, G. K. Ma, and Q. Li, *J. Compos. Mater.* **173-178**, 50 (2016).
- [9] J. Li, H. W. Zhang, Y. N. Liu, Y. L. Liao, G. K. Ma, and H. Yang, *Mater Res Express*, **2** (2015).
- [10] J. F. Wang, D. Chen, W. Wu, L. Wang, and G. C. Liang, *T. Nonferr. Metal. Soc.* **2239-2248**, 27 (2017).
- [11] S. Bierlich, F. Gellersen, A. Jacob, and J. Topfer, *Mater. Res. Bull.* **19-23**, 86 (2017).
- [12] S. Taufeeq, A. Parveen, S. Agrawal, and A. Azam, *Dae. Solid. State. Phys. Sym.* **2015**, 1731 (2016).
- [13] D. Chen, Y. Liu, Y. Li, W. Zhong, and H. Zhang, *J. Magn. Magn. Mater.* **2837-2840**, 323 (2011).
- [14] R. C. Pullar, *Prog. Mater. Sci.* **1191-1334**, 57 (2012).
- [15] A. K. Pradhan, P. R. Mandal, K. Bera, S. Saha, and T. K. Nath, *Phys. B.* **1-6**, 525 (2017).
- [16] C. L. Huang and Y. C. Chen, *J. Eur. Ceram. Soc.* **167-173**, 23 (2003).
- [17] Z. L. Zheng and H. W. Zhang, *IEEE. T. Magn.* **4230-4233**, 49 (2013).
- [18] C. C. Liu, X. S. Liu, S. J. Feng, K. M. U. Rehman, M. L. Li, C. Zhang, H. H. Li, and X. Y. Meng, *J. Supercond. Nov. Magn.* **933-937**, 31 (2018).
- [19] J. Li, S. He, K. Z. Shi, Y. Wu, H. Bai, Y. Hong, W. J. Wu, Q. X. Meng, D. C. Jia, and Z. X. Zhou, *Ceram. Int.* **6953-6958**, 44 (2018).